PNAS
www.pnas.org

Supplementary Information for

Biased μ-opioid analgesics derived from a novel tetrapeptide class found in an Australian fungus

Z. Dekan, S. Sianati, A. Yousuf, K.J. Sutcliffe, A. Gillis, C. Mallet, P. Singh, A.H. Jin, A.M. Wang, S.A. Mohammadi, M. Stewart, R. Ratnayake, F. Fontaine, E. Lacey, A. Piggott,Y.P. Du, M. Canals, R.B. Sessions, E. Kelly, R.J. Capon, P.F. Alewood, M.J. Christie.

Corresponding author Macdonald J Christie
Email: mac.christie@sydney.edu.au

This PDF file includes:

Supplementary Text

Supplementary Methods

Peptide isolation, characterization and synthesis

General isolation and synthetic details (bilaids A-C): Initial HPLC was performed on a system consisting of two Shimadzu LC-8A Preparative Liquid Chromatographs with static mixer, Shimadzu SPD-M10AVP Diode Array Detector and Shimadzu SCL-10AVP System Controller. Further HPLC was performed using an Agilent 1100 Series separations module equipped with Agilent 1100 Series diode array and/or multiple wavelength detectors, Polymer Laboratories PL-ELS1000 ELSD and Agilent 1100 Series fraction collector and running ChemStation (Revisions 9.03A or 10.0A). NMR spectra were acquired in DMSO-d_6 on a Bruker Avance 500 or a Bruker Avance 600 spectrometer under XWIN-NMR or Topspin control, referenced to residual ^{1}H signals. Electrospray ionization mass spectra (ESIMS) were acquired using an Agilent 1100 series separations module equipped with an Agilent 1100 series LC/MSD mass detector and Agilent 1100 series diode array detector. High-resolution (HR) ESIMS measurements were obtained on a Finnigan MAT 900 XL-Trap instrument with a Finnigan API III source. Unless otherwise specified, a constant level of 0.1% TFA was used in all HPLC separations. Chiroptical measurements ($[\alpha]_D$) were obtained on a Jasco P-1010 Intelligent Remote Module type polarimeter in a 100 × 2 mm cell.

Fmoc-L- and D-amino acids were obtained from Novabiochem (Laufelfingen, Switzerland) or Peptide Institute (Osaka, Japan). 2-Chlorotrityl chloride and Rink-amide resins were purchased from Novabiochem (Laufelfingen, Switzerland). 2-(1*H*-benzotriazol-1-yl)-1,1,3,3-tetramethyluronium hexafluorophosphate (HBTU) was obtained from Richelieu Biotechnologies (Quebec, Canada). Trifluoroacetic acid (TFA), *N*,*N*-diisopropylethylamine (DIEA) and *N*,*N*-dimethylformamide (DMF), all peptide synthesis grade, were purchased from Auspep (Melbourne, Australia).

Extraction and isolation of bilaids: The strain MST-MF667 was isolated from a boat ramp on the Huon estuary, Port Huon, Tasmania, Australia. The previous phenotypic description of MST-MF667 as a strain of *Penicillium bilaii*[1] has been refined by genomic analysis as a new species adjacent to *Penicillium bilaiae*. (**Supplementary Figure S1**). A solid phase culture (200 × 15 g petri dishes, 21 days, 24 °C) of MST-MF667 on Malt Extract Agar [malt extract (16%), peptone (0.8%), glucose (16%), agar (2%)] was extracted with MeOH (2 × 2 L) and the combined extract concentrated *in vacuo* to an aqueous residue (~ 400 mL). The aqueous residue was in turn extracted with EtOAc (3 × 400 mL) and the combined fractions concentrated *in vacuo* (14.9 g) prior to being partitioned between petroleum spirit (200 mL) and 20% H_2O/MeOH (200 mL). A portion (1.2 g) of the aqueous MeOH soluble material was subjected to preparative HPLC (1 injection, Phenomenex Luna C_{18} column, 150 × 21.2 mm, 5 µm, 5 mL/min, gradient elution from 90% H_2O/MeOH to 100% MeOH with a constant 0.05% TFA/MeOH modifier, over 180 min) to afford ten fractions. Fraction 6 (129 mg) was subjected to preparative HPLC fractionation (4 injections, Agilent Zorbax SB-C_{18} column, 250 × 21.2 mm, 7 µm, 21.2 mL/min gradient elution from 50% H_2O/MeOH to 20% H_2O/MeOH with a constant 0.01% TFA/H_2O modifier, over 50 min) to yield bilaid A (**1a in Supplementary Table 1**) (22.8 mg, 0.15%). Fraction 5 was subjected to preparative HPLC fractionation (7 injections, Agilent Zorbax SB-C_{18} column, 150 × 21.2 mm, 5 µm, 20 mL/min gradient elution from 75% H_2O/MeCN to 30% H_2O/MeCN with a constant 0.05% TFA/H_2O modifier, over 30 min) followed by semi-preparative HPLC (Agilent Zorbax SB-CN column, 250 × 9.4 mm, 5 µm column, 4 mL/min isocratic elution at 25% H_2O/MeCN + 0.1% TFA/H_2O) to yield bilaid B (**2a in Supplementary Table 1**) (265 µg, 0.0018 %) and bilaid C (**3a in Supplementary Table 1**) (121 µg, 0.0008 %). [Note: All % yields were calculated as an estimated weight to weight percentage present in the aqueous MeOH soluble material (1.2 g)].

Bilaid A (FvVf-OH) (1a). light brown oil; $[\alpha]_D$ +9 (c 0.2, 0.1% TFA/MeOH); HRESI(+)MS *m/z* 533.2745 [(M+Na), $C_{28}H_{38}N_4O_5Na$ requires 533.2740]. NMR (DMSO-d_6) data for natural and synthetic bilaid A:

	natural bilaid A[a]		synthetic bilaid A[b]	
	δ_H, mult (*J* in Hz)	δ_C	δ_H, mult (*J* in Hz)	δ_C
L-Phe				
1		168.0		167.9
2	4.24, br dd (*7.5, 7.0*)	53.2	4.26, br s	53.1
3a	3.04, dd (*13.7, 7.5*)	37.5	3.04 dd (*13.8, 7.1*)	37.4
3b	2.93, dd (*13.7, 8.2*)		2.94, dd (*13.8, 8.1*)	
4		134.8		134.8
5,9	7.15 – 7.35, m	129.4	7.15 – 7.33, m	129.4
6,8	7.15 – 7.35, m	128.4	7.15 – 7.33, m	128.4
7	7.15 – 7.35, m	127.0	7.15 – 7.33, m	127.0
D-Val				
1		170.1		170.1
2	4.51, m	56.9	4.55, dd (*9.2, 5.1*)	56.6
2-NH	8.40, d (*9.1*)		8.48, d (*9.1*)	
3	1.84, m	31.3	1.83, m	31.5
4	0.67, m	17.1	0.66, d (*6.9*)	17.1
5	0.67, m	18.9	0.61, d (*6.9*)	18.9
L-Val				
1		170.5		170.6
2	4.31, dd (*9.0, 5.7*)	56.7	4.32, dd (*9.2, 5.6*)	56.7
2-NH	8.04, d, (*9.3*)		8.11, d (*9.3*)	
3	1.77, m	30.7	1.72, m	30.9
4	0.64, m	19.1	0.62, d (*6.9*)	19.1
5	0.52, d (*6.6*)	17.1	0.47, d (*6.8*)	17.1
D-Phe				
1		172.9		173.0
2	4.48, m	53.3	4.47, ddd (*8.6, 4.6, 2.0*)	53.3
2-NH	8.32, d (*8.4*)		8.42, d (*8.4*)	
3a	3.08, dd (*14.2, 4.6*)	37.0	3.08, dd (*13.8, 4.5*)	36.9
3b	2.81, dd (*13.7, 10.3*)		2.78, dd (*13.8, 10.7*)	
4		137.4		137.4
5,9	7.15 – 7.35, m	129.0	7.15 – 7.33, m	129.0
6,8	7.15 – 7.35, m	128.0	7.15 – 7.33, m	128.0
7	7.15 – 7.35, m	126.3	7.15 – 7.33, m	126.3

[a] (500 MHz, DMSO-d_6) [b] (600 MHz, DMSO-d_6)

Bilaid B (FvVy-OH) (2a). light brown oil; HRESI(+)MS *m/z* 549.2692 [$(M+Na)^+$, $C_{28}H_{38}N_4O_6Na$ requires 549.2689]. NMR data (600 MHz, DMSO-d_6) for natural and synthetic bilaid B:

	natural bilaid B	synthetic bilaid B	
	δ_H, mult (*J* in Hz)	δ_H, mult (*J* in Hz)	δ_C
D-Phe			
1			168.1
2	4.23, m	4.26, dd, (*8.2*, *6.9*)	53.2
3a	3.05, m	3.04, dd, (*13.8*, *6.8*)	37.5
3b	2.94, m	2.93[a], dd, (*13.8*, *8.3*)	
4			135.0
5,9	7.29 – 7.35, m	7.29 – 7.33, m	129.5
6,8	7.29 – 7.35, m	7.29 – 7.35, m	128.5
7	7.24 – 7.28, m	7.24 – 7.26, m	127.5
L-Val			
1			170.2
2	4.55, m	4.54, dd, (*9.1*, *5.1*)	56.9
2-NH	8.47, d, (*8.9*)	8.47, d, (*9.2*)	
3	1.84, m	1.84, m	31.5
4	0.68, m	0.67[a], d	17.2
5	0.65, m	0.63, d, (*6.8*)	19.0
D-Val			
1			170.7
2	4.32, dd, (*9.5*, *5.5*)	4.33, dd, (*9.3*, *5.7*)	56.7
2-NH	8.14, d, (*9.1*)	8.12, d, (*9.3*)	
3	1.79, m	1.80, m	31.0
4	0.67, m	0.66[a], d	19.3
5	0.55, d, (*6.8*)	0.54, d, (*6.9*)	17.3
L-Phe			
1			173.3
2	4.37, m	4.37, m	53.7
2-NH	8.30, brs	8.33, d, (*8.3*)	
3a	2.95, m	2.96[a], dd, (*13.8*, *4.2*)	36.3
3b	2.67, m	2.68, dd, (*13.9*, *10.1*)	
4			127.1
5,9	7.00, d, (*8.4*)	7.00, d, (*8.5*)	130.0
6,8	6.63, d, (*8.4*)	6.63, d, (*8.5*)	114.9
7			156.0

[a] resonances overlapping

Bilaid C (YvVf-OH) (3a). light brown oil; HRESI(+)MS *m/z* 527.2879 [$(M+H)^+$, $C_{28}H_{39}N_4O_6$ requires 527.2870]. NMR data (600 MHz, DMSO-d_6) for synthetic bilaid C:

	synthetic bilaid C	
	δ_H, mult (*J* in Hz)	δ_C
L-Tyr		
1		168.2
2	4.14, dd, (*7.8, 6.9*)	53.5
3a	2.94, dd, (*14.0, 7.7*)	36.8
3b	2.80, m	
4		124.9
5,9	7.08, d, (*8.5*)	130.5
6,8	6.69, d, (*8.4*)	115.3
7		156.6
D-Val		
1		170.2
2	4.55, dd, (*9.1, 5.2*)	56.8
2-NH	8.45, d, (*9.1*)	
3	1.86, m	31.6
4	0.70, d, (*6.9*)	17.3
5	0.69, d, (*6.8*)	19.1
L-Val		
1		170.7
2	4.32, dd, (*9.2, 5.6*)	56.7
2-NH	8.12, d, (*9.3*)	
3	1.73, m	30.9
4	0.62, d, (*6.8*)	19.2
5	0.49, d, (*6.8*)	17.1
D-Phe		
1		173.1
2	4.54, m	53.4
2-NH	8.40, d, (*8.3*)	
3a	3.08, dd, (*13.8, 4.5*)	37.0
3b	2.77, m	
4		137.6
5,9	7.22 – 7.26, m	129.1
6,8	7.22 – 7.26, m	128.1
7	7.16 – 7.19, m	126.4

Co-metabolites encountered in *Penicillium* sp. MST-MF667 include citromycin, citromycetin, (–)-2,3-dihydrocitromycin, (–)-2,3-dihydrocitromycetin, *cyclo*-(L-Pro-L-Tyr), *cyclo*-(L-Pro-L-Val), *cyclo*-(L-Phe-L-Pro), *cis*-bis(methylthio)silvatin, pistillarin and bilains A-C.[1]

Marfey's analyses: To a sample (500 µg) of **1** was added 6 M HCl (500 µL) and the resulting solution heated at 110 ºC for 17 h. The HCl was then left to boil off at 100 ºC. To samples (approx. 50 µg) of **2** and **3** was added 6 M HCl (100 µL) and the resulting solution heated at 100 ºC for 19 h. The HCl was then removed under N_2 gas. To the hydrolyzed material of **1a** was added H_2O (50 µL), 1 M sodium bicarbonate (20 µL) and 1% 1-fluoro-2,4-dinitrophenyl-5-L-alaninamide (L-FDAA) in acetone (100 µL). The solution was heated at 37 ˚ C for 1 h, neutralized with 1 M HCl (20 µL) and diluted with MeCN (810 µL). The hydrolyzed materials of **2a** and **3a** were treated in an identical manner but using half the volume of reagents and solvents. HPLC analysis involved elution of 5 µL of the derivatized solutions through a Zorbax SB-C_{18} or SB-C_8 column, 150 × 4.6 mm, 5 µm, 1 mL/min, gradient of 15 – 45% MeCN / 0.1 M aqueous ammonium acetate adjusted to pH 3 with TFA over 45 min and UV detection at 340 nm. Co-injections with authentic derivatized amino acids were carried out using the above conditions.

Fmoc protection of natural bilaid A (1a). A sample of **1a** (500 µg, 1 eq.) was dissolved in 1:1 H_2O:THF (500 µL). To this was added $NaHCO_3$ (92 µg, 1.1 eq.) in H_2O (10 µL), *N*-(9-fluorenylmethoxycarbonyloxy)succinimide (371 µg, 1.1 eq.) in 1:1 H_2O:THF (100 µL) and the reaction sealed and left at 30 ºC for 19 h. All solvents were removed under N_2 gas, and the sample dissolved in MeOH (250 µL). An aliquot (100 µL) was purified by analytical HPLC (2 × 50 µL injections, Zorbax Eclipse C_8 column, 250 × 9.4 mm, 5 µm, 1 mL/min with a gradient elution of 10 – 100% MeCN / H_2O (+ isocratic 0.01% TFA)/MeCN over 15 min, with the product eluting at 12.7 min.

Acid hydrolysis and Marfey's analysis on Fmoc protected bilaid A (1a). To the purified protected peptide was added 6 M HCl (200 µL) and the resulting solution heated at 110 ºC

for 19 h. The HCl was removed under N_2 gas. Marfey's reaction was carried out in an identical manner as for **1**. HPLC analysis was as for **1a**.

Structure elucidation of bilaid A: High resolution ESI(+)MS analysis of bilaid A (**1**) revealed a pseudo molecular ion (M+Na) consistent with a molecular formula ($C_{28}H_{38}N_4O_5$ Δmmu = +0.5) requiring twelve double bond equivalents (DBE). The ^{1}H NMR (DMSO-d_6) data for **1a** featured three amide protons and four α-methines, consistent with a linear tetrapeptide, while interpretation of the 2D NMR data afforded the sequence Phe-Val-Val-Phe-OH. Marfey's analysis on **1a** confirmed equimolar amounts of L-Val, D-Val, L-Phe and D-Phe. *N*-protection of a sample of **1a** with Fmoc, followed by Marfey's analysis resulted in diminished levels of the D-Phe derivative, positioning D-Phe at the C-terminus, and by inference L-Phe at the N-terminus. To unambiguously complete the structure elucidation of **1** all four possible stereoisomers were synthesized: namely bilaid A (FvVf-OH, **1a**) fVvF-OH (**1b)**, FVvf-OH (**1c**), and fvVF-OH, (**1d**). HPLC analysis of the purified synthetic tetrapeptide stereoisomers on a Zorbax SB-C_8 analytical column confirmed common retention times for the enantiomeric pairs **1a**/**1b** (8.0 min) and **1c**/**1d** (6.8 min), with co-injection studies confirming that bilaid A co-eluted **1a/1b**. Chiral HPLC was used to resolve **1a** (6.8 mins) from **1b** (5.7 mins) and unambiguously confirm the structure for bilaid A (**1a**) as shown in **Fig. 1**.

Isolation of bilaids B and C (2a and 3a): Having identified bilaid A (**1a**), we re-examined the MST-MF667 fermentation extract in an effort to detect additional, related linear tetrapeptides. A more detailed HPLC-DAD-ESI(±)MS analysis of both polar and non-polar fractions succeeded in detecting two additional linear tetrapeptides, bilaid B (**2a**) and bilaid C (**3a**), as minor co-metabolites. High resolution ESI(+)MS analysis of **2a** and **3a** revealed that they were isomeric, with pseudo molecular ions (M+Na) consistent with a molecular formula ($C_{28}H_{38}N_4O_6$, Δmmu +0.3 and +0.9), as mono-oxygenated homologues of **1a**. The ^{1}H NMR (DMSO-d_6) data for **2a** and **3a** was very similar to that for **1a** and supported replacement of one Phe residue with a Tyr residue. A Marfey's analysis carried out on **2a** and **3a** revealed the presence of L-Phe, D-Val, L-Val and D-Tyr in **2a** and L-Tyr, D-Val, L-Val and D-Phe in **3a**. Given the structure assignment made above for **1a** we hypothesized

that **2a** and **3a** were the isomeric tetrapeptides FvVy-OH and YvVf-OH respectively. To test this hypothesis, we prepared synthetic standards which proved to be chromatographically and spectroscopically identical with the natural products. Thus, the structures for bilaids B (**2a**) and C (**3a**) were assigned as shown in **Fig. 1**.

General peptide synthesis procedure (bilaids A-C): All peptides were assembled manually by stepwise solid-phase peptide synthesis. 2-Chlorotrityl chloride resin (0.176 g, 0.25 mmol; for peptide acids) or Rink amide resin (0.176 g, 0.25 mmol; for peptide amides) was swollen in DMF for 2 h and drained. The first Fmoc protected amino acid (1 mmol) was dissolved in DMF (2 mL) and DIEA (174 µL, 1 mmol) was added. After complete dissolution of the amino acid, the mixture was added to the reaction vessel and shaken for 2 h. The resin was flow washed with DMF for 1 min. The Fmoc protecting group was removed by shaking the resin with 5% piperidine/DMF mixture (2 × 10 mL, each cycle for 1 min). After deprotection the resin was again flow washed for 1 min. The next amino acid (1 mmol) was activated with 0.5 M HBTU solution (2 mL) and DIEA (174 µL, 1 mmol) and was added to the reaction vessel. The mixture was shaken for 10 min and a ninhydrin test was performed to calculate the coupling yield. This test was repeated after each coupling. After completion of the assembly, the terminal Fmoc group was removed as described above, the resin washed with DMF followed by DCM and dried under nitrogen. The peptide was cleaved from the resin by shaking with 10 mL of cleavage mixture (95% TFA / 5% water) for 2 h. TFA was evaporated under N_2 gas.

Purification of synthetic peptide acids from solid phase synthesis: Reaction products for the synthetic peptides, were purified by preparative HPLC (Zorbax SB-C_{18} column, 250 × 21.2 mm, 7 µm, isocratic 45% H_2O(0.1% TFA): MeOH for bilaid A (FvVf-OH, 35.3 mg) (**1a**) and fVvF-OH, 41.0 mg (**1b**); 30% H_2O(0.1% TFA):MeOH for FVvf-OH, 25.0 mg (**1c**) and fvVF-OH, 30.8 mg (**1d**); 40% H_2O(0.1% TFA); bilaid B (FvVy-OH, 44.8 mg) (**2a**) and bilaid C (YvVf-OH, 45.9 mg) (**3a**).

Solution conversion of tetrapeptide acids to amides: To a solution of di-*tert*-butyl-dicarbonate in 1,4-dioxane (29.3 mg/mL) was added pyridine (10.5 µL/mL) and

ammonium bicarbonate (10.5 mg/mL). To selected tetrapeptides was added 300 – 600 µL (4 equivalents). After stirring for 3 days at 50 ºC, the reaction products were purified by preparative HPLC (Zorbax SB-C_{18} 250 × 21.2 mm column; isocratic; 40% H_2O (0.1% TFA).

LC/MS analyses on natural and synthetic peptides: Performed on Zorbax SB-C_8 150 × 4.6 mm, 5 µm column (flow 1 mL/min; gradient 10 – 100% MeCN / H_2O (+ isocratic 0.05% HCO_2H) over 15 min.

Chiral HPLC analysis on natural and synthetic peptides: Performed on Astec Chirobiotic T column, 150 × 4.6 mm, 5 µm, 0.5 mL/min, isocratic MeOH (0.1% triethylamine, 0.2% AcOH, pH 6.23).

General analytical and synthetic methods (bilorphin and bilactorphin): RP-HPLC solvent A was 0.05% TFA / H_2O and solvent B was 0.043% TFA / 90% acetonitrile / H_2O. Analytical HPLC was performed on a Shimadzu LC20AT system using a Thermo Hypersil GOLD C18 2.1 × 100 mm column at flow rate of 0.3 mL / min. Absorbance was recorded at 214 nm. Preparative HPLC was performed on a Waters DeltaPrep 3000 system using a Vydac 208TP 50 × 250 mm column at a flow rate of 80 mL / min. Mass spectra were recorded in positive ionization mode on an API 2000 triple quadrupole mass spectrometer (AB SCIEX, Framingham, MA, USA). Fmoc amino acids and O-(1H-benzotriazol-1-yl)-1,1,3,3-tetramethyluronium hexafluorophosphate (HBTU) were from Iris Biotech (Marktredwitz, Germany), dimethylformamide (DMF) and diisopropylethylamine (DIEA) were from Auspep (Melbourne, Australia). Boc-2,6-dimethyl-L-tyrosine was purchased from AstaTech Inc (Bristol PA, USA). All other reagents were obtained from Sigma Aldrich.

N^{α}-(9-fluorenylmethoxycarbonyl)-3-*O*-[2,3,6-tri-*O*-acetyl-4-*O*-(2,3,4,6-tetra-*O*-acetyl-β-D-galactopyranosyl)-β-D-glucopyranosyl]-L-serine (Fmoc-L-Ser[β-Lac(OAc_7)]-OH)

β-lactose peracetate was prepared according to the procedure outlined by Xu et al.[2] Briefly, α-lactose monohydrate (20.0 g) was added in portions to a stirring suspension of sodium acetate (5.0 g) in acetic anhydride (200 mL) with the temperature maintained at 135 °C. After 1 h the solution was poured into ice-water (1 L) and stirred overnight. The resulting precipitate was collected by filtration, redissolved in CH_2Cl_2, washed with satd. $NaHCO_3$ and dried over $MgSO_4$. Following removal of solvent under reduced pressure it was crystallized from CH_2Cl_2 / MeOH (16.1 g, 42%). ESI-MS (*m/z*): calc. 619.2 $[M\text{-}OAc]^+$ found 619.3.

Fmoc-L-Ser-OH was O-β-lactosylated based on the procedure described by Salvador et al.[3] To a mixture of β-lactose peracetate (5.0 g) and Fmoc-L-Ser-OH (2.9 g) in anhydrous CH_2Cl_2 (100 mL) was added BF_3•Et_2O (2.8 mL) and stirred under nitrogen for 20 h. The solution was washed with 1 M HCl then water and dried over $MgSO_4$. Purified by silica gel chromatography (1% AcOH / 2% MeOH in CH_2Cl_2) followed by RP-HPLC (50% B isocratic) (1.9 g, 27% from β-lactose peracetate). ESI-MS (*m/z*): calc. 946.3 $[M+H]^+$ found 946.3.

H-[2,6-dimethyl-L-tyrosyl]-D-Val-L-Val-D-Phe-L-Ser(β-Lac)-NH_2 (bilactorphin, 3g)

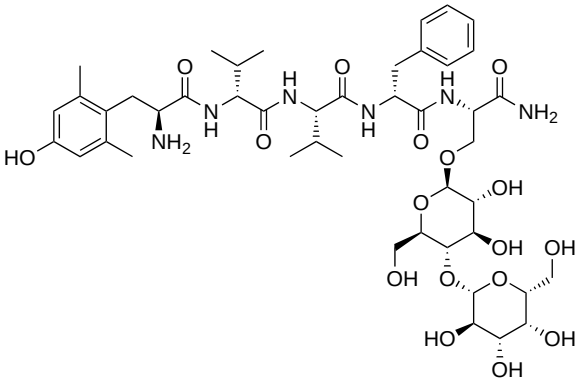

Peptide assembly was perfomed using Fmoc chemistry on 0.5 mmol scale on Fmoc-Rink-amide polystyrene resin (substitution value 0.67 mmol/g). Fmoc deprotections were accomplished by treatments with 50% piperidine / DMF (2 × 1 min). Couplings were performed using three equivalents of Fmoc amino acid / HBTU / DIEA (1:1:1) relative to resin loading (30 min). Fmoc-O-β-lactosyl-L-serine was incorporated as the hepta-O-acetate (prepared as described above); Boc-2,6-dimethyl-L-tyrosine was used without side-

chain protection. Cleavage from the resin and removal of side-chain protecting groups was achieved by treatment with 95% TFA / 2.5% TIPS / 2.5% H_2O for 2 h at room temperature. TFA was removed under a stream of nitrogen, and the product was precipitated using cold diethyl ether / n-hexane (1:1), washed with Et_2O, redissolved in 50% acetonitrile / 0.1% TFA / H_2O and lyophilized. ESI-MS (*m/z*): calc. 1259.5 $[M+H]^+$, found 1259.7. The crude product was deacetylated by treatment with a solution of 5% hydrazine / 30% acetonitrile / H_2O for 5 h then purified by RP-HPLC (10 to 50% B over 40 min). (190 mg, 39% from initial resin loading). ESI-MS (*m/z*): calc. 965.5 $[M+H]^+$, found 965.4.

***In vitro* Pharmacology.**

Receptor binding assays: Receptor binding assays were performed under contract by Cerep/Eurofins (France). Briefly, binding of [^{3}H]DAMGO to human recombinant MOPr (hMOPr) stably expressed in HEK-293 (Human Embryonic Kidney) cell line was performed as previously described.[4] Briefly [^{3}H]DAMGO (0.5 nM) was incubated with hMOPr expressing membranes for 120 min at 22 °C and separated by rapid filtration prior to liquid scintillation counting. Non-specific binding was defined in the presence of 10 μM naloxone. Inhibition of specific binding by various concentrations of peptides was determined and fitted using GraphPad Prism 7.02 software. Similarly inhibition of binding to human recombinant DOPr (hDOPr) expressed in CHO (Chines Hamster Ovary) cell line was performed using incubation with [^{3}H]DADLE (0.5 nM) for 120 min at 22 °C, and Similarly binding to human recombinant KOPr (hKOPr) expressed in CHO (Chines Hamster Ovary) cell line was performed using incubation in [^{3}H]U-69593 (2 nM) for 60 min at 22 °C.

cAMP Assays: cAMP assays were performed under contract by Tetra-Q Pty Ltd (Brisbane QLD Australia) Briefly, detection of cAMP was based on the competition between intracellular cAMP and biotinylated cAMP linked streptavidin-coated donor beads for anti-cAMP conjugated acceptor beads. Donor and acceptor proximity was detected as emission at 520-620 nm. Inhibition of forskolin (10 μM) stimulated cAMP levels were determined for each test peptide at a concentration of 10 μM.

Brain slice electrophysiology: Brain slices containing locus coeruleus LC neurons were prepared from male Sprague Dawley rats (4-6 weeks) as described previously.[5] Briefly, male rats were anesthetized with isoflurane and decapitated. The brain was dissected and mounted in a vibratome chamber (Leica biosystem, VT100, Wetzlar, Germany) in order to prepare horizontal brain slices (280 μm). Slices were cut and stored in warm (34°C) artificial cerebrospinal fluid (ACSF) containing the following (in mM): 125 NaCl, 2.5 KCl, 2 $CaCl_2$, 1 $MgCl_2$, 1.25 NaH_2PO_4, 25 $NaHCO_3$, 11 glucose and 0.01 (+) MK801 (95% O_2 - 5% CO_2). Slices were incubated in warm oxygenated ACSF for at least 30 min before recording. Slices were transferred to the recording chamber while warm ACSF (34°C) was superfused at a rate of ~2 mL/min. Whole-cell voltage-clamp recordings were acquired from LC neurons with Multiclamp 700B amplifier (Molecular Devices, CA, USA) at holding potential of - 60 mV. Recording pipettes (2-4 MΩ) were filled with internal solution containing (in mM): 135 K gluconate, 8 NaCl, 10 HEPES, 0.5 EGTA, 2 Mg- ATP and 0.3 Na-GTP; pH 7.3, 280-285 mOsM. Continuous current recordings were collected in chart mode at 500 Hz and filtered at 20 - 50 Hz using Axograph X (Axograph Scientific, Sydney, Australia). Series resistance monitored throughout the experiments and remained < 15 MΩ; otherwise the data were discarded. Outward current was measured as the difference between baseline current and peak current of drug application.

Expression of MOPr in AtT20 cells: Wild type mMOPr was cloned in pcDNA3.1 plasmids with FLAG-tag and expressed stably in AtT20 cells at a deliberately low level of MOPr expression (8 pmol/mg protein; 2 x 10^5 receptors/cell estimated from cytometry) as previously described.[6] For patch clamp experiments AtT20 cells were seeded on 35 mm polystyrene culture dishes (Beckton, Dickinson Biosciences) in Dulbecco modified Eagle medium (Gibco, Life Technologies, Australia) containing 4.5 g/L glucose, penicillin-streptomycin (100 μL/mL), G418 (50mg/mL) (Gibco, Invitrogen) and 10% FBS. Cell cultures were kept in humidified 5% CO_2 atmosphere at 37°C. Cells were ready for recording after 24 hours incubation.

Expression of GRK2-YFP and β-arrestin 2-HA in AtT20

GRK2-YFP and β-arrestin 2-HA plasmids were transfected using TurboFect (Thermo Fisher Scientific) onto mMOPr expressing AtT20 cells according to manufacturer's instructions, 24 h after plating on glass coverslips in 35 mm tissue culture dishes. After serum starving plated cells, for every 3 mL reaction volume 4 µg of GRK2-YFP and 4 µg of β-arrestin 2-HA DNA was diluted into 400 µL serum free Opti-MEM (Gibco, Life Technologies, Australia) followed by 6 µL of TurboFect. Solution was mixed and added dropwise onto dishes after 15 min room temperature incubation. Media was changed at 24 h with transfection assessed by YFP fluorescence and experiments were conducted 48 h after transfection.

Ser 375 Phosphorylation assay: AtT20 cells stably expressing MOPr were grown on coverslip to ~50% confluence. Cells were serum starved for at least 30 min and then incubated in the absence or presence of the indicated ligand for 5-10 min at 37°C. Phosphorylation was terminated by fixing the cells with -30°C methanol followed by 10 min incubation on ice. Cells were washed three times with phosphate buffered saline (PBS) and then heated in sodium citrate buffer (10 mM, 0.05% Tween 20, pH.6) for 20 min at 95°C. Cells were incubated with anti-phospho Ser 375 antibody (1:200, Cell Signaling) overnight at room temperature. Next day, labeled receptors were stained with Alexa-fluor 488 antibody (1µg/mL, 1 h at room temperature, Thermo Fisher Scientific). Imaging was performed as detailed below.

Arrestin recruitment: Agonist-induced recruitment of β-arrestin2 to MOPr was examined using a BRET-based approach. AtT20 cells were plated in 10-cm dishes and co-transfected with MOPr C-terminally tagged with Rluc8 (MOPr-RLuc8), β-arrestin2-YFP and GRK2 (1, 4 and 2 µg, respectively). 24h after transfection wells were replated into white opaque 96-well plates (CulturPlate, PerkinElmer) and allowed to adhere overnight. Cells were washed with Hank's Balanced Salt Solution (HBSS) and equilibrated in HBSS for 30 min at 37°C prior to the experiment. Coelenterazine h was added to a final concentration of 5 µM 10 min before dual fluorescence/luminescence measurement in a LUMIstar Omega plate reader (BMG LabTech). Baseline BRET was measured for 30 sec prior to addition of

the indicated ligand. The BRET signal was calculated as the ratio of light emitted at 530 nm by YFP over the light emitted at 430 nm by *Renilla* luciferase 8 (RLuc8).

Endocytosis assay: Receptor internalization was quantified using a ratiometric staining of membrane and internalized receptors. Briefly, AtT20 cells expressing FLAG-tagged MOPr were incubated with 1 μg/mL Alexa594-conjugated M1 monoclonal anti-FLAG (prepared from Alexa-fluor 594 with a succinimidyl ester moiety, Molecular Probes) for 30 min to label membrane receptors. Cells were then incubated for an additional 30 min with indicated agonist at 37°C. To unbind the M1 anti-FLAG antibody from the surface receptors, cells were quickly washed three times with ice-cold PBS lacking Mg^{2+} and Ca^{2+} and supplemented with 0.04% EDTA (pH 7.4). Cells were fixed with 4% paraformaldehyde in PBS for 20 min under non-permeabilized condition and then were incubated with anti-FLAG polyclonal antibody (1 μg/ml, 2 h at room temperature, Sigma Aldrich) followed by Alexa-fluor 488 goat anti-rabbit antibody (1μg/ml, 1 h at room temperature, Thermo Fisher Scientific). Therefore, surface receptors were labeled with Alexa-fluor 488, while internalized receptors were labeled with Alexa-fluor 594. Percentage of internalized receptors was calculated as a ratio of mean 594 nm fluorescence intensity to total mean fluorescence intensity at 594 nm and 488 nm.

In experiments where GRK2-YFP and β-arrestin 2-HA were expressed, Alexa-fluor 405 goat anti-rabbit (2 μg/mL, 1 h at room temperature, Abcam) was used as a secondary antibody in place of Alexa-fluor 488 goat anti-rabbit to avoid fluorescence spectral overlap with YFP. 405 nm fluorescence was false-colored to green for representative images. Only YFP positive cells were analyzed for internalization.

Imaging: Images of receptor phosphorylation and internalization were acquired using Zeiss 510 Meta laser scanning confocal microscope at a resolution of 1024 × 1024 pixels using a 60× oil emulsion objective. Imaging parameters including laser intensity, photomultiplier tube (PMT) voltage and offset remained constant for each experiment. Mean fluorescence intensity was measured using ImageJ software to calculate mean gray value of an area defined outside a single cell. Each experiment was normalized to the mean

of untreated cells as 0% and the mean of cells treated with saturating concentrations of Met-enk (30 μM) as 100%.

Cultured cell electrophysiology: Perforated patch clamp recordings were performed as previously described (Yousuf et al., 2015).[7] Pipettes were pulled from borosilicate glass (AM Systems, Everett, WA, USA) yielding input resistances between 3.5 - 4.5 MΩ and were filled with internal solution containing 135 mM potassium gluconate, 3 mM $MgCl_2$, 10 mM HEPES (adjusted to pH 7.4 with KOH). The recording electrodes were first front filled with this internal solution and then backfilled with the same solution containing 200 μg/mL amphotericin B (in 0.8% DMSO). For measuring I_{GIRK} the KCl concentration in the bath was increased to 20 mM (substituted for NaCl) before the start of the measurements and was maintained throughout the experiments as previously described in Yousuf et al. (2015).[7] Liquid junction potential was calculated to be +16 mV and was adjusted before the start of each recording. Currents were recorded at 37°C in a fully enclosed, temperature-controlled recording chamber using an Axopatch 200B amplifier and pCLAMP 9.2 software, and digitized using Digidata 1320 (Axon Instruments, Molecular Devices, Sunnyvale, CA, USA). Currents were sampled at 100 Hz, low pass filtered at 50 Hz and recorded on hard disk for later analyses. I_{GIRK} was recorded using a 200 ms voltage step to - 120 mV from a holding potential of - 60 mV delivered every 2 s. Drugs were perfused directly onto cells using a ValveLink 8.2 pressurized pinch valve perfusion system (AutoMate Scientific, USA).

Data Analyses: All data are shown as the mean ± SEM and analyzed using GraphPad Prism v7. All data points are plotted as chord GIRK conductance (G_{GIRK}, nS) using the following calculation: [I_{GIRK} (- 60 mV) - I_{GIRK} (- 120 mV)] pA / 60 mV.

Bias calculation and statistics: Agonist concentration response curves were fitted to a three-parameter concentration response curve, a logistic function with constrained slope of 1, in GraphPad Prism 7 producing estimates of curve location (EC_{50}) and asymptote (E_{max}). As basal activity was subtracted in all pathways the bottom of the curve was constrained to 0.

The de facto standard for quantifying agonist affinity and efficacy to accurately determine biased signaling is the operational model of agonism.[8,9] Agonist concentration response data for each pathway was fitted to the operational model. Maximal effect in the system was defined by the reference full-agonist met-enkephalin and the slope of the transducer curve constrained to one. Efficacy (τ) and affinity (KA) estimates were produced from the curve fit for test agonists endomorphin-2, bilorphin and morphine. log(τ/KA) values for each agonist were normalized by subtraction of the reference agonist met-enkephalin log(τ/KA) value within each pathway to produce Δlog(τ/KA). Subtraction across pathways produced $\Delta\Delta$log(τ/KA), a normalized estimated of each agonist's signaling bias. Previous papers on the operational model have advocated application of pooled variance in order to increase the power of these comparisons.[10] This approach is not suitable here, or in any situation with variable curve fit quality, due to the very low signaling efficacy of the biased agonists producing much larger error for the fit derived parameters and invalidating the assumptions of pooled variance (**Supplementary Table 2**). Standard error of the linear combinations of parameters was therefore propagated exactly under standard rules.[11] Poor curve fit due to low signaling efficacy reduced the power of the $\Delta\Delta$log(τ/KA) approach generally and prevented confident interpretation of bias estimates from this approach (**Fig. S2E**).

In cases where all test agonists are partial compared to the reference agonist efficacy alone has been used to quantify bias.[12] In systems with low receptor reserve the asymptote of the logistic function, E_{max}, is a robust, assumption free and affinity independent estimate of efficacy that approaches the value of operational efficacy. In systems with a linear relationship between agonist occupancy and effect such as the β-arrestin pathways studied here where there is no signal amplification, E_{max} approximates operational efficacy, 'τ'.

Here, we normalized E_{max} to the reference agonist within each pathway and subtracted across comparison pathways to produce Δ normalized E_{max}, an efficacy measure of bias. Observation of concentration-response curve position, which approaches operational

affinity for all partial agonists presented here, across pathways measured shows bias in this instance does not appear affinity driven due to conservation of rank potency.

Degrees of freedom were calculated by first conservatively taking the lower of the two sample sizes when normalizing to met-enkephalin. In the case of Δ normalized E_{max}, variance across the pathways could be assumed to be equal allowing degrees of freedom to be summed. In the case of ΔΔlog(τ/KA), low efficacy in the ß- pathways caused heterogeneity of variance and degrees of freedom was approximated using the Welch-Satterwaite equation (ISO/IEC Guide to Uncertainty in Measurement).

Bias of each agonist, in both Δ normalized E_{max} and ΔΔlog(τ/KA) calculations, was tested by a one-way t-test to 0, the value of the reference agonist. The bias of bilorphin was then compared to morphine using a two-sample t-test, equal or unequal variance as appropriate. All comparisons were multiplicity adjusted using the Holm-Sidak ranking method (GraphPad Prism 7) within each pair of pathways examined.

Molecular dynamics

Generation of peptide conformations: The 3D conformers of bilorphin and endomorphin-2 (EM2) were built in Chimera.[13] Two endomorphin-2 conformers were used, with the Tyr1-Pro2 peptide bond modelled as either the cis or trans isomer, and treated as separate ligands for MD simulation and docking. Peptides were protonated at the N-terminal tyrosine and parameterized with Antechamber and the general Amber force field.[14,15] To account for the flexibility of the tetrapeptides, conformer generation was performed by running 1 μs MD simulations of each peptide in explicit solvent (0.15 M NaCl and TIP3P water) under the Amber ff14SB force field. These trajectory data were analyzed with cpptraj[16] to extract 10,000 conformations for each peptide to use in molecular docking.

Docking of peptides to MOPr: Molecular docking was performed with the Bristol University Docking Engine (BUDE).[17] Peptides were docked to an inactive MOPr model obtained from the x-ray crystal structure of the antagonist-bound MOPr (PDB: 4DKL).[18]

The protein was prepared in Insight II (Accelrys) as follows; ligands and the T4 lysozyme were removed, and a loop search performed to find a homologous loop to model in the missing intracellular loop 3. A loop was selected by visual inspection and the residues changed to the correct mouse MOPr sequence. Molecular docking to this MOPr structure was performed with each of the three peptides, bilorphin, cis-endomorphin-2 and trans-endomorphin-2, independently. The following describes the docking procedure for one peptide. Multi-conformer docking was run such that the 10,000 conformations of the peptide were treated as independent molecules. A box of size 15, 15, 15 Å centered on the orthosteric binding site was designated as the search space. BUDE's genetic algorithm was used to search the available pose space for the best energy poses. A total of 105,000 poses were sampled for each of the 10,000 peptide conformers. The total possible number of poses was 1.57×10^8 for each conformer, corresponding to x,y,z translation within the box and 360˚ rotation in all axes in 10˚ increments. The 50 lowest energy binding poses were inspected visually and subjected to a distance constraint between the protonated amine of the ligand and Asp147$^{3.32}$ of less than 3 Å. The selected peptide-MOPr complexes were used in short (125 ns) MD simulations to assess the stability of the binding pose, before a full 1 μs of trajectory data was collected, as described below. Based on the docking data and the initial 125 ns MD simulations, the cis-endomorphin-2 conformer was chosen for further simulation.

MD simulations: Each peptide-MOPr complex was embedded in a POPC:POPE:cholesterol lipid bilayer at a 5:5:1 ratio using the replacement method, and the simulation box (initial dimensions: 90, 110, 90 Å) solvated with TIP3P water and NaCl (150 mM), using the CHARMM-GUI software.[19] Amber parameter topology and coordinate files were prepared in LEaP. Structures were minimized over 10,000 steps, then the system was heated under constant volume and pressure with lipids restrained, from 0 K to 100 K over 5 ps, and then from 100 K to 310 K over 100 ps. 10 rounds of 500 ps equilibration was performed under constant pressure to equilibrate the periodic box dimensions. Simulations were run in 8 x 125 ns parallel steps under the Amber ff14SB and Lipid14 force fields,[20,21] producing 1 μs of simulation data for each peptide-MOPr complex. Temperature and pressure were controlled using the Langevin thermostat and the

anisotropic Berendsen barostat, with a 2 fs time step and trajectories written every 100 ps. Trajectories were visualized in VMD,[22] analysis was performed using cpptraj, [16] and images were prepared in Chimera.[13]

Principal Component Analysis: Trajectories were aligned to a set of "core residues" showing the least fluctuation during the simulation time to remove general translation and rotation of the protein in analysis. Principal component analysis was performed on the 3D Cartesian coordinates of the alpha carbons of the transmembrane domains of all trajectories, yielding 567 eigenvalues. Receptor conformations at each simulation time point were projected onto the first 2 PCs, accounting for ~40 % of the variance.

Nociception testing

All experiments involving animals were approved by the University of Sydney Animal Ethics Committee (AEC. Protocol number K00/12-2011/3/5650). Experiments were performed under the guidelines of the Australian code of practice for the care and use of animals for scientific purposes (National Health and Medical Research Council, Australia, 7th Edition). Great care was taken to minimize animal suffering during these experiments and to reduce the number of animals used. Adult male C57BL/6 mice (20 - 25 g) were housed 5 - 6 per cage in individually ventilated cages under controlled light (12:12 h, lights on at 6am) and climate (18 - 23°C, 40 - 60% humidity) conditions. Food and water was available *ad libitum*. Mice were given at least 7 days to habituate to housing facilities prior to handling, and handled by the experimenter for 4 days prior to testing. Experiments were conducted between 8am and 6pm in a quiet, temperature-controlled room (21 ± 1°C). The experimenter was blind to all drugs tested. Animals were tested on a 54°C hotplate, with a maximum cut-off time of 20 seconds to prevent tissue damage. Endpoints were hindpaw lick, hindpaw flutter or jump. Baseline latency was recorded immediately before subcutaneous injection with morphine, bilactorphin or vehicle (20% PEG400/saline v/v) in a total volume of 200 µL. Mice were tested 30, 60, 90, 150, 210, 330 and 450 min following injection. The percentage of maximal possible effects (%MPE) were calculated as follows: %MPE = (test latency – baseline latency)/(cutoff latency – baseline latency) x 100%. The cut-off latency was 20 seconds. Significant differences were assessed with a two-way

ANOVA and Tukey's post hoc multiple comparisons test. The dose-response curves for bilactorphin and morphine were calculated using the maximal responses for each dose between 30-90 min. Doses were transformed to the logarithm of μmol/kg. A two-way ANOVA was used to compare data at equimolar doses.

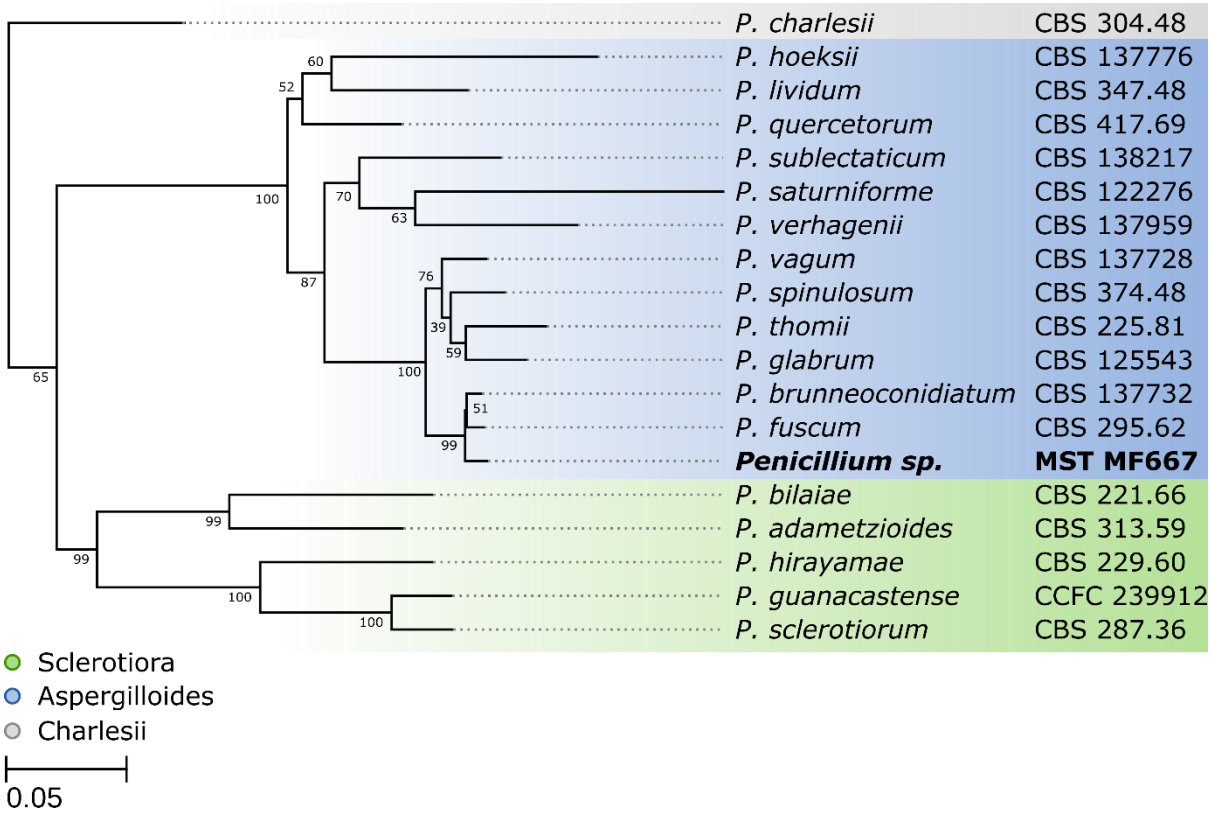

Fig. S1. Maximum Likelihood (ML) tree for *Penicillium* sp. MST-MF667: Inferred from a concatenated dataset of partial gene sequences for the (a) Internal Transcribed Spacer (ITS) region, (b) beta-tubulin gene (BenA) and (c) calmodulin gene (CaM). Tree was constructed using RAxML-ng under the General Time Reversible model with gamma-distributed rate heterogeneity and a proportion of invariant sites (GTR+I+G). Branch support values are derived from 1000 bootstrap replicates.

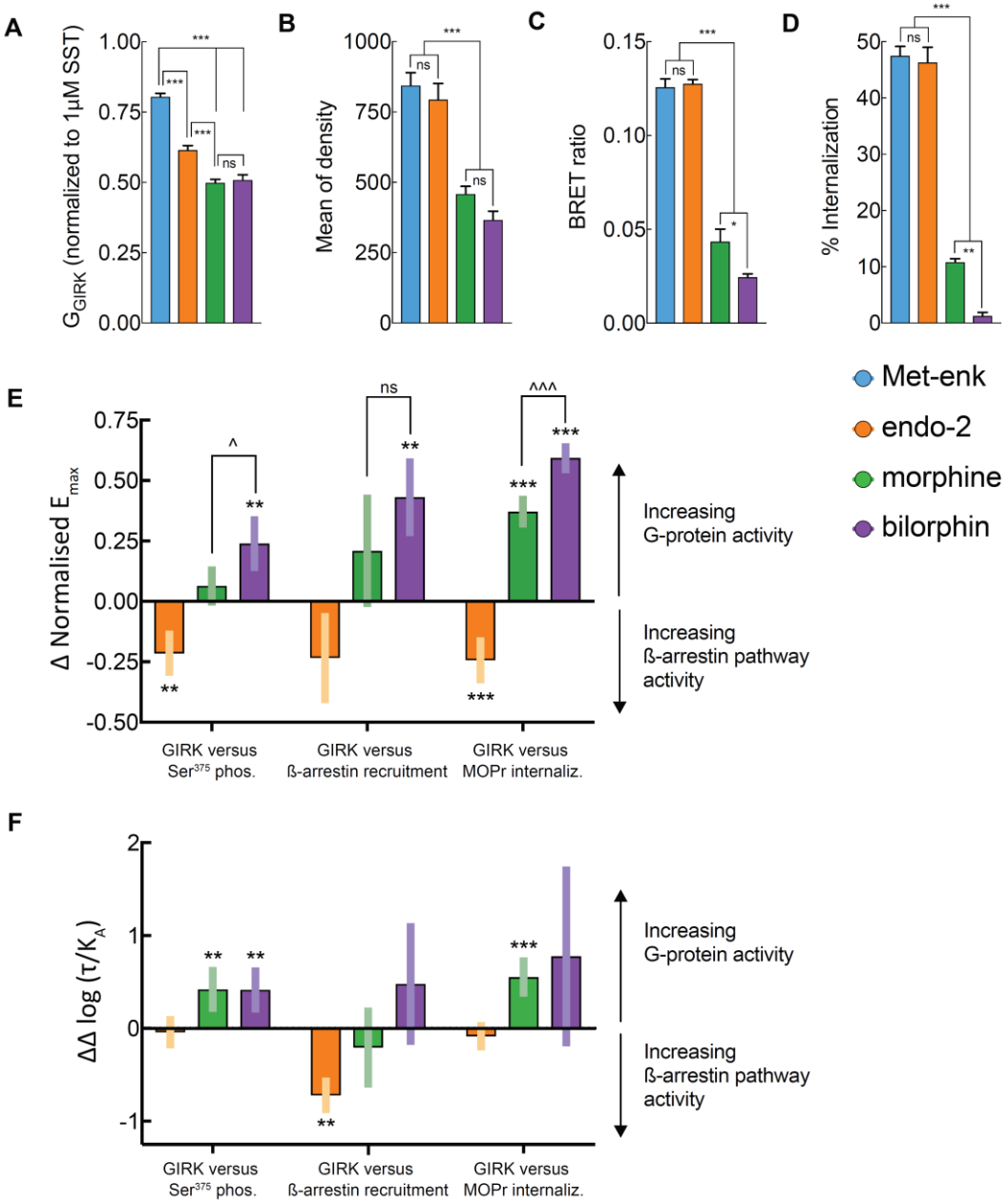

Fig. S2. Maximal effect of agonists in each signaling and calculation of bias for G-protein activation versus other pathways: Non-normalized maximal efficacy data (± S.E.M.) for activation of **A**. GIRK, **B**, Ser^{375} phosphorylation, **C** β-arrestin 2 recruitment and **D** internalization that was used to calculate ratios presented in Figure 3 (A-D: * $P < 0.05$, ** $P < 0.01$, *** $P < 0.001$ for indicated contrasts), and for calculation of Δ Normalized E_{max} in **E**, or included in the operational model in **F**. All data represented in **E** and **F** are mean with 95% confidence intervals (E, F: * $P < 0.05$, ** $P < 0.01$, *** $P < 0.001$ versus 0.00; $^{\Lambda}$ $P < 0.05$, $^{\Lambda\Lambda\Lambda}$ $P < 0.001$ for indicated contrasts).

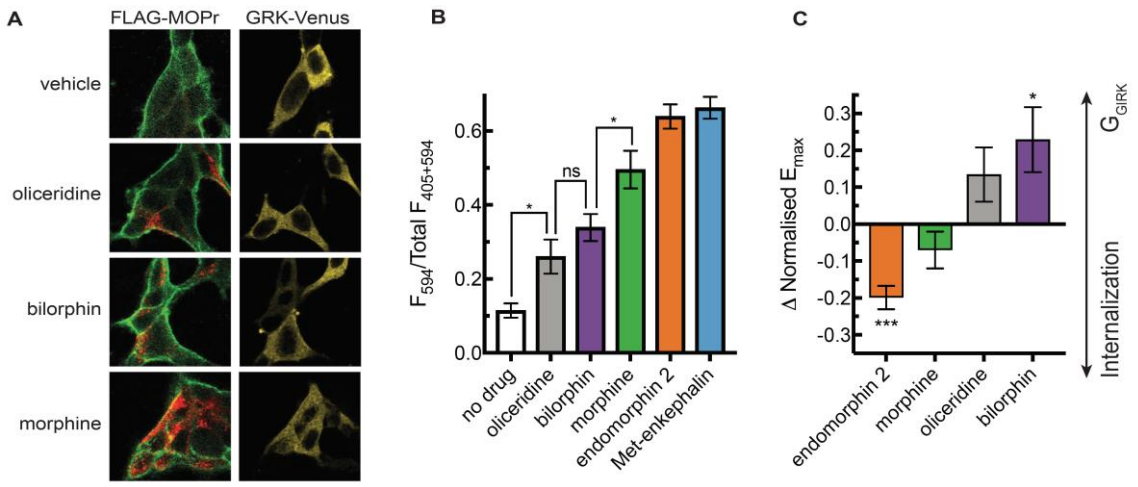

Fig. S3. A. Example images of enhanced internalisation of FLAG-MOPr (green and red as in Fig 3) produced by oliceridine, bilorphin or morphine in cells overexpressing both GRK2-Venus (yellow) and ß- arrestin 2. **B**. Internalization of each agonist (ratio of fluorescence in red/[green + red] chanels) in cells transiently transfected with GRK2-Venus and ß–arrestin 2 (n = 5 experiments, with greater than ten cells in each, * $P < 0.05$). **C**. Bias ratios calculated from G_{GIRK} maxima normalized to Met-enk (from Fig. 2E) and enhanced internalization (from Fig. S3A) normalized to Met-enkeph for bilorphin indicates greater G- protein bias than both oliceridine and morphine.

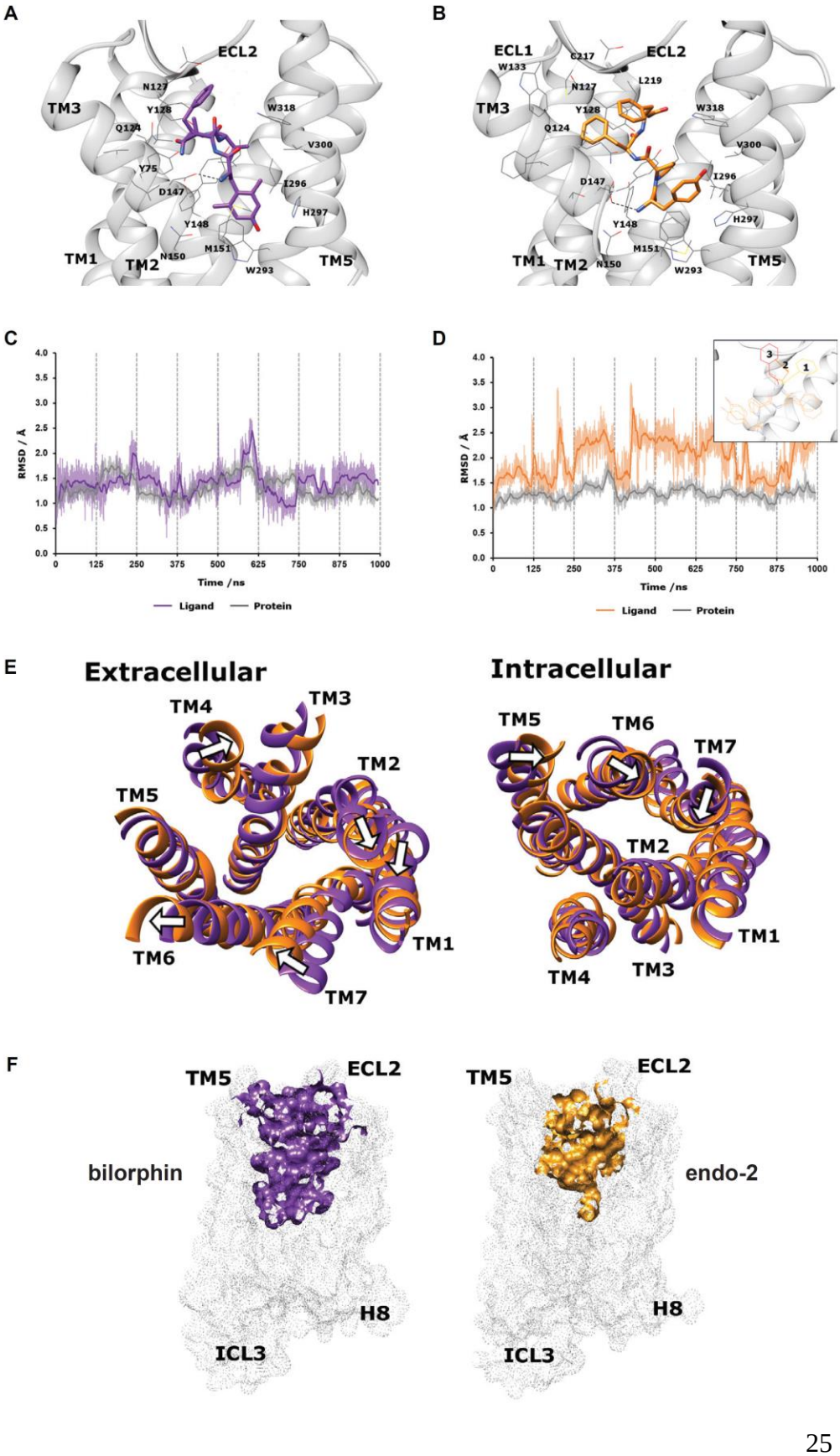
A
ECL2
TM3
N127
Y128
Q124
W318
V300
Y75
D147
I296
H297
Y148
M151
TM1
TM2
N150
W293
TM5
B
ECL1
ECL2
C217
W133
L219
N127
TM3
Y128
W318
Q124
V300
D147
I296
H297
Y148
M151
TM1
TM2
N150
W293
TM5
C
RMSD / Å
Time /ns
Ligand
Protein
D
RMSD / Å
Time /ns
Ligand
Protein
E
Extracellular
TM4
TM3
TM2
TM5
TM1
TM6
TM7
Intracellular
TM5
TM6
TM7
TM2
TM1
TM4
TM3
F
TM5
ECL2
bilorphin
H8
ICL3
TM5
ECL2
endo-2
H8
ICL3

Fig. S4. Molecular Dynamics simulations: A. Alternative viewpoint from Figure 4A of the predicted binding poses of bilorphin (purple), and **B**. endomorphin-2 (orange), and the positions of the surrounding binding pocket residues (grey) obtained after molecular docking and 1 μs of MD simulations. The salt bridge between protonated amine of the ligands and Asp1473.32 is marked as a dashed black line. TM4 has been removed for clarity. **C**. RMSD calculations performed on the heavy atoms of bilorphin, compared to the initial docked pose (purple), and the alpha carbons of the receptor transmembrane domains, compared to the first frame of the MD simulation (grey). **D.** RMSD calculations performed on the heavy atoms of endomorphin-2, compared to the initial docked pose 24 (orange), and the alpha carbons of the receptor transmembrane domains, compared to the first frame of the MD simulation (grey). Inset: fluctuations of Phe4 in endomorphin-2 during the MD simulation showing 3 different positions of Phe4 . **E**. Following principal component analysis performed on the alpha carbons of the MOPr transmembrane domains, extracted structures representing the extremes of PC1 demonstrate the conformational differences between the bilorphin – MOPr complex (purple) and the endomorphin-2 – MOPr complex (orange). Loops have been removed from the image to depict only the part of the receptor the principal component analysis was performed on. White arrows indicate conformational changes in the helices moving from bilorphin – bound to endomorphin-2 – bound MOPr. **F**. Calculation of the volume of the orthosteric binding site using CASTp showed the binding pocket was larger for the bilorphin – MOPr complex (purple) compared to the endomorphin-2 – MOPr complex (orange). CASTp calculations were performed on structures averaged over the final 100 ns of each simulation. Receptors are viewed in the plane of the membrane.

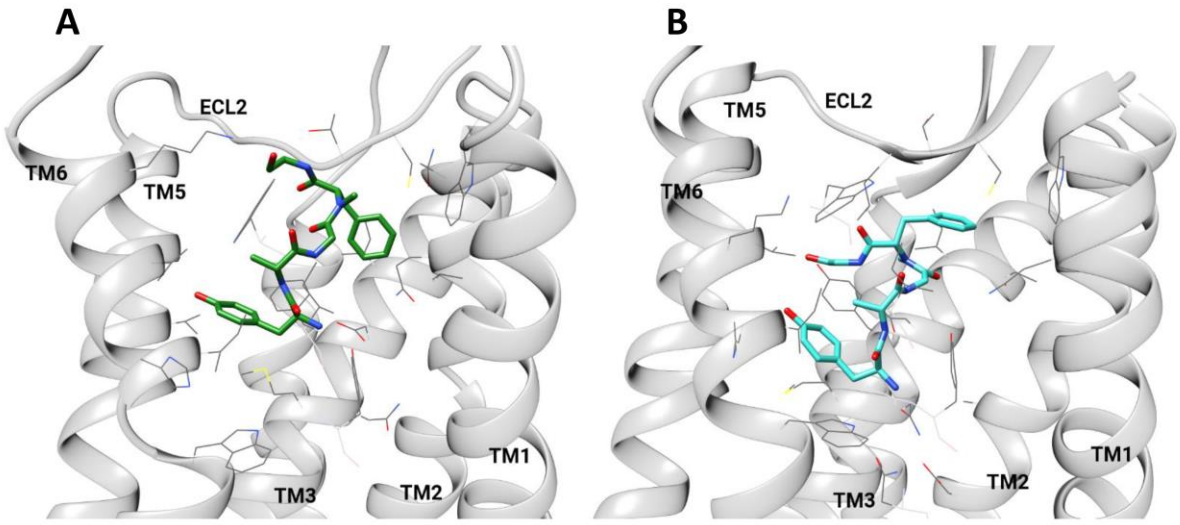

Fig. S5. Cryo-EM structure and Molecular Dynamics simulations with DAMGO: A. The binding pose of DAMGO in the cryo-EM structure of the MOPr-G_i complex.[42] DAMGO is shown in green, with surrounding binding pocket residues and the receptor helices in grey. **B.** Our predicted binding pose of DAMGO after docking with BUDE and 1 μs MD simulation starting from the inactive MOPr structure;[1] DAMGO is shown in cyan and surrounding residues and helices in grey. Koehl *et al* (2018)[42] reported poor resolution of the C-terminal portion of DAMGO and high flexibility of this region in an MD simulation. With this flexible C-terminal ethanolamine omitted, the RMSD between all heavy atoms of DAMGO in the cryo-EM structure and in our final pose after 1 μs MD was 2.83 Å. Thus the DAMGO-MOPr interactions in the cryo-EM structure and our model were virtually identical.

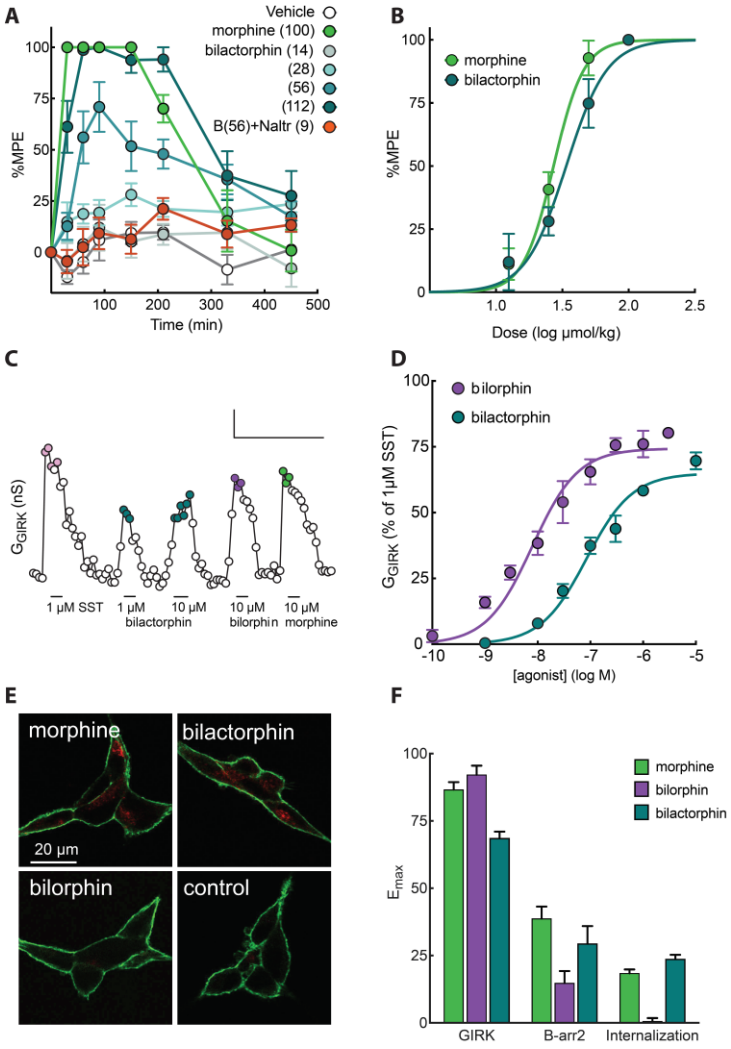

Fig. S6. Antinociceptive properties and bias of bilactorphin: Bilactorphin (**3g**) is analgesic *in vivo* but loses some bias properties of bilorphin (**3c**). **A.** Subcutaneous bilactorphin produced dose-dependent analgesia in mice on the 54°C hotplate, and was antagonized by naltrexone. Doses in µmol/kg (n = 7-12 per data point except naltrexone [n = 4]). **B.** Peripherally administered bilactorphin was equipotent with morphine (n = 5-12). **C.** Representative trace of G_{GIRK} in MOPr expressing AtT20 cell in response to bilorphin and bilactorphin, and morphine relative to a probe of 1 µM somatostatin. The scale bars represent 0.2 ns and 1 min. **D.** Concentration response curves of G_{GIRK} induced by bilorphin and bilactorphin normalized to the response to 1 µM somatostatin. **E.** MOPr internalization induced by 30 µM bilorphin and bilactorphin (membrane and internalized MOPr in green and red respectively). **F.** Maximal efficacy values of morphine, bilorphin and bilactorphin relative to Met-enkephalin (30 µM exposure to each agonist).

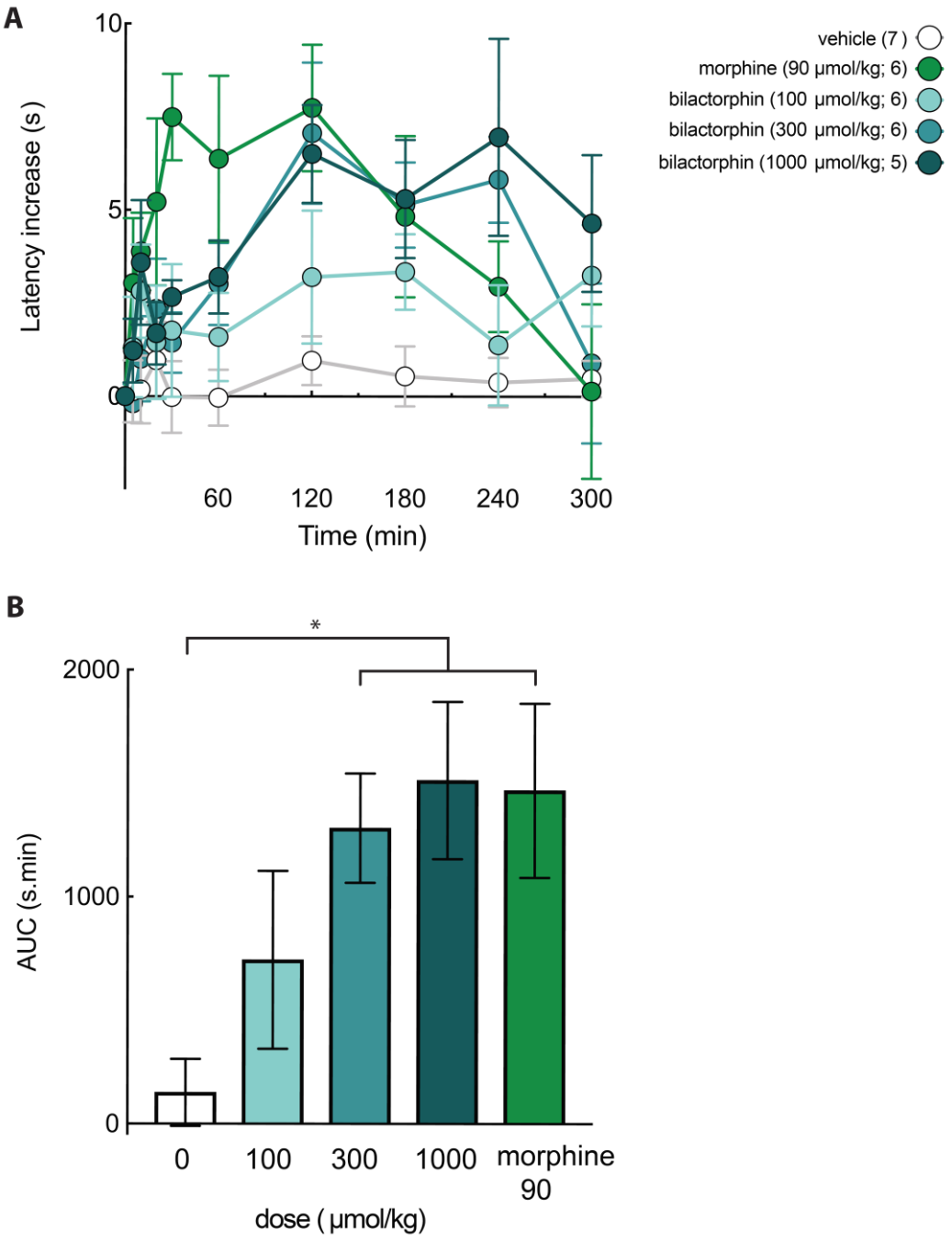

Fig. S7. Antinociceptive action of oral bilactorphin and morphine: A. Time-response (mean ± SEM) for oral gavage of bilactorphin and morphine on hot-plate latency. **B.** Area under the curve (AUC) of the full time-response data over 5 hours for each animal shown in **A** for 300 min after gavage. Ordinary one-way ANOVA of AUC data revealed statistically significant differences between all doses of bilactorphin above 100 µmol/kg and morphine 90 µmol/kg (* $P < 0.05$).

Supplementary references

1. Capon, R.J., Stewart, M., Ratnayake, R., Lacey, E. & Gill, J.H. Citromycetins and bilains A-C: new aromatic polyketides and diketopiperazines from Australian marine-derived and terrestrial Penicillium spp. *J Nat Prod* **70**, 1746-52 (2007).
2. Xu, P., Yang, J.Y. & Kováč, P. Observations on the Preparation of β-Lactose Octaacetate. *Journal of Carbohydrate Chemistry* **31**, 711-720 (2012).
3. Salvador, L.A., Elofsson, M. & Kihlberg, J. Preparation of building blocks for glycopeptide synthesis by glycosylation of Fmoc amino acids having unprotected carboxyl groups. **51**, 5643-5656 (1995).
4. Wang, J.B. et al. Human mu opiate receptor. cDNA and genomic clones, pharmacologic characterization and chromosomal assignment. *FEBS Lett* **338**, 217-22 (1994).
5. Sadeghi M., Tzschentke T.M. & Christie M.J. μ-Opioid receptor activation and noradrenaline transport inhibition by tapentadol in rat single locus coeruleus neurons. *Br J Pharmacol.* **172**, 460-8 (2015).
6. Borgland, S.L., Connor, M., Osborne, P.B., Furness, J.B. & Christie, M.J. Opioid agonists have different efficacy profiles for G protein activation, rapid desensitization, and endocytosis of mu-opioid receptors. *J Biol Chem* **278**, 18776-84 (2003).
7. Yousuf, A. et al. Role of Phosphorylation Sites in Desensitization of μ-Opioid Receptor. *Mol Pharmacol* **88**, 825-35 (2015).
8. Black, J.W. & Leff, P. Operational models of pharmacological agonism. *Proc R Soc Lond B Biol Sci* **220**, 141-62 (1983).
9. Kenakin, T. The Effective Application of Biased Signaling to New Drug Discovery. *Mol Pharmacol* **88**, 1055-61 (2015).
10. Kenakin, T., Watson, C., Muniz-Medina, V., Christopoulos, A. & Novick, S. A simple method for quantifying functional selectivity and agonist bias. *ACS Chem Neurosci* **3**, 193-203 (2012).
11. Farrance, I. & Frenkel, R. Uncertainty of Measurement: A Review of the Rules for Calculating Uncertainty Components through Functional Relationships. *Clin Biochem Rev* **33**, 49-75 (2012).
12. Burgueño, J. et al. A Complementary Scale of Biased Agonism for Agonists with Differing Maximal Responses. *Sci Rep* **7**, 15389 (2017).
13. Pettersen, E.F. et al. UCSF Chimera-a visualization system for exploratory research and analysis. *J Comput Chem* **25**, 1605-12 (2004).
14. Wang, J., Wang, W., Kollman, P.A. & Case, D.A. Automatic atom type and bond type perception in molecular mechanical calculations. *J Mol Graph Model* **25**, 247-60 (2006).
15. Wang, J., Wolf, R.M., Caldwell, J.W., Kollman, P.A. & Case, D.A. Development and testing of a general amber force field. *J Comput Chem* **25**, 1157-74 (2004).
16. Roe, D.R. & Cheatham, T.E. PTRAJ and CPPTRAJ: Software for Processing and Analysis of Molecular Dynamics Trajectory Data. *J Chem Theory Comput* **9**, 3084-95 (2013).
17. McIntosh-Smith, S., Price, J., Sessions, R.B. & Ibarra, A.A. High performance *in silico* virtual drug screening on many-core processors. *Int J High Perform Comput Appl* **29**, 119-34 (2015).

18. Manglik, A. et al. Crystal structure of the μ-opioid receptor bound to a morphinan antagonist. *Nature* **485**, 321-6 (2012).
19. Jo, S., Kim, T., Iyer, V.G. & Im, W. CHARMM-GUI: a web-based graphical user interface for CHARMM. *J Comput Chem* **29**, 1859-65 (2008).
20. Maier, J.A. et al. ff14SB: Improving the Accuracy of Protein Side Chain and Backbone Parameters from ff99SB. *J Chem Theory Comput* **11**, 3696-713 (2015).
21. Dickson, C.J. et al. Lipid14: The Amber Lipid Force Field. *J Chem Theory Comput* **10**, 865-879 (2014).
22. Humphrey, W., Dalke, A. & Schulten, K. VMD: visual molecular dynamics. *J Mol Graph* **14**, 33-8, 27-8 (1996).